ELSEVIER

Physica C 320 (1999) 65–70

PHYSICA C

Tunable detection of radiation from HTSC Josephson junction arrays

Kiejin Lee [a,*], Ienari Iguchi [a], Karen Y. Constantinian [b]

[a] *Department of Applied Physics, Tokyo Institute of Technology and CREST, Japan Science and Technology (JST), Oh-okayama, Meguro-ku, Tokyo, 152-8551 Japan*

[b] *Institute of Radioengineering and Electronics RAS, Mokhovaya 11, Moscow, 103907 Russian Federation*

Received 5 February 1999; received in revised form 15 April 1999; accepted 27 April 1999

Abstract

We have investigated the mutual phase interaction between a single detector junction and a phase-locked three-junction array of high-T_c Josephson junctions. The YBCO Josephson junctions were fabricated on a MgO bicrystal substrate. We measured the radiation power of a Josephson-junction array using an off-chip coupled to a radiometer and on-chip coupled to a single junction from centimeter- to millimeter-wave ranges. The Josephson oscillation power excited the resonant mode coupled to the coplanar microstrip loops. Clear self-induced Shapiro steps were observed in the current–voltage curves of the detector junction. The power transfer to the single detector junction was estimated from the modulation of the Shapiro step height. The maximum detected power level was about 7 nW at frequency 150–250 GHz.

Keywords: HTSC Josephson junctions; Critical current; Voltage

1. Introduction

High-T_c superconducting (HTSC) Josephson junctions have the possibility that the oscillation of the Josephson ac current can be used for a practical voltage-controlled microwave oscillator and a sensitive detecting device for millimeter and submillimeter wavelengths. Possible applications include tunable integrated local oscillators and pumps for Josephson mixers. Because of the large energy gap of HTSC Josephson junctions, high frequency applications up to THz frequency range can be expected [1,2]. However, a single HTSC $YBa_2Cu_3O_y$ (YBCO) Josephson junction did not produce sufficiently large coherent radiation power with narrow linewidth necessary for direct use in various microwave devices. These problems may be overcome by using coherent arrays of phase locked junctions [3,4]. Recently, some promising results have been obtained from the HTSC SNS-type Josephson junction arrays with high resistance detector junctions and bicrystal Josephson junction arrays [5–8]. The phase-locking of Josephson junction array having series-parallel geometry with the pair of junctions shunted by superconducting loops was demonstrated in a previous report [8]. The junction array showed coherent radiation over the wide range of frequencies and the best perfor-

* Corresponding author. Tel.: +81-357-34-2454; fax: +81-357-34-2751; E-mail: klee@htsc.ap.titech.ac.jp

0921-4534/99/$ - see front matter
PII: S0921-4534(99)00292-0

mance of the array could be obtained by modulating the external small magnetic field. In this paper, we measured the microwave radiation power of a Josephson-junction array using an off-chip coupled to a radiometer and an on-chip coupled to single junction from centimeter- to millimeter-wave ranges. Using an on-chip coupling measurement, clear self-induced Shapiro steps were observed in the current–voltage characteristics of the detector junction. We have investigated the mutual phase-locking between a detector junction and a three-junction array where each junction is enclosed in a coplanar microstrip resonator. We used YBCO bicrystal junctions on a MgO bicrystal substrate. The junction array where the bias leads formed a coplanar microstrip resonator was phase-locked by means of a dc SQUID geometry. The geometry of array junction is independent of the spread in the critical current which is a critical problem for the HTSC Josephson oscillator. For the off-chip emission measurements, we compared the microwave radiation power of the detector junction and the three-junction array.

2. Experimental setup

The radiation power from the junction array was measured by a superheterodyne detection technique with a non-resonant broad-band matching system at receiving frequencies $f_{REC} = 11$, 22, 36, 47 and 72 GHz. The receiver was operated in a two band regime with a bandwidth $\Delta B = 2$ GHz. The sensitivity of the receiver was $\delta S \approx 3 \times 10^{-24}$ W/Hz at an integrating time $\tau = 1$ s. The absolute value of the self-radiation power emitted from the junctions was exactly calibrated by a standard noise source installed inside the microwave receiver system.

3. Layout and fabrication

The YBCO superconducting thin films were deposited on MgO bicrystal substrates (24°) by laser ablation technique and patterned into an array of three junctions by the conventional photolithography method. In order to avoid the large critical current (I_c), the thickness of YBCO films was chosen to be about 50 nm. Note that, for the single YBCO bicrystal junction with the film thickness of about 50 nm and the junction width of about 10 μm, I_c and normal resistance R_n were usually about 300 μA and 0.4–0.80, at 4.2 K, respectively. The photograph of the circuit and equivalent circuit of the three-junction array and the two detector junctions are shown in Fig. 1. The three-junction array and the two detector junctions were located at the center of coplanar strip lines which were 10 μm wide with 10 μm pitch as shown in Fig. 1(a). For this circuit structure, two separate detector junctions of (a) and (b) and one oscillator junction of the three-junction array can be biased separately. For the array design, pairs of bicrystal junctions were shunted by superconducting SQUID loops whose magnetic induc-

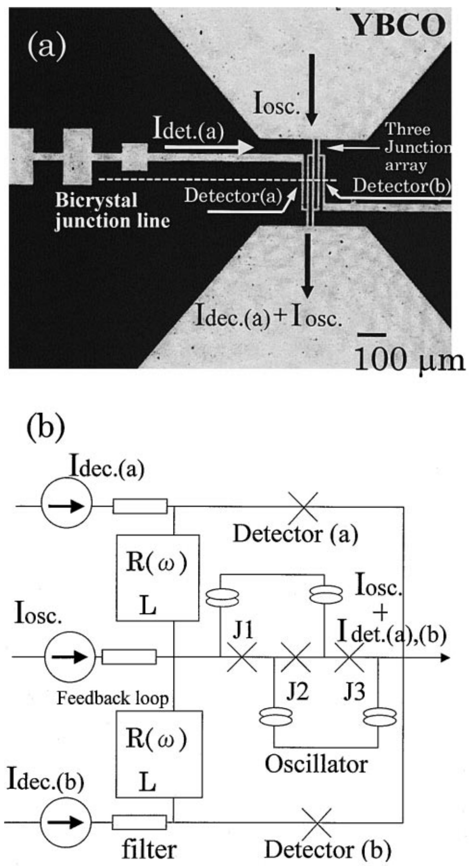

Fig. 1. (a) Photograph and (b) equivalent circuit of the YBCO of the three-junction array and the two-detector junctions on a bicrystal substrate. The three bicrystal junctions locate at the center of the microstrip lines.

tance was about 0.2 nH with a mutual inductance between the loops of about 17 pH. Note that, in such a SQUID-type junction array the distribution of the inductance in the coupling loop should be taken into account, because the locking strength depends on the loop inductance. In principle the inductance should be large enough and the mutual inductance between the SQUIDs must be small enough to make the junctions oscillate in phase and to reduce the dependence of the relative phases on the flux through the SQUID loops, where the external impedance would be $Z = j\omega L$. The inductance of the loop was chosen to make the junction impedance equal to 60 Ω at about 100 GHz operating frequency. The array structure consisted of two series of interlocking dc SQUIDs. The dc-bias supply produces opposite but equal dc voltages between adjacent bridges, thus all the junctions oscillate at the same average frequency corresponding to the basic Josephson voltage–frequency relation $f = V/\Phi_0$, where f is the oscillation frequency, V is the voltage of the junction and Φ_0 is the flux quantum. After electrical testing of the junction-array and the detector junction, a 500 nm thick SiO dielectric layer was evaporated over the array to isolate the junctions from a 500 nm thick Au feedback loop. The sample was magnetically shielded by superconducting Pb and μ-metal.

4. Results and discussion

Before testing the mutual phase interaction between two junctions, we separated our device and tested the microwave properties of the detector junction and the array which could be separately biased. In Table 1 we present the characteristic parameters of the two detector junctions and the array. The characteristic values of the $I_c R_n$ product are comparable for both junctions. The I_c of the array junction

Table 1
Parameters of $YBa_2Cu_3O_y$ three-junction array oscillator and detector junctions at 4.2 K

	I_c (mA)	R_N (Ω)	$I_c R_n$ (mV)	T_c (K)
Detector (a)	0.63	0.74	0.47	87
Detector (b)	0.68	0.5	0.34	87
Three-junction array	1.45	0.3	0.43	87

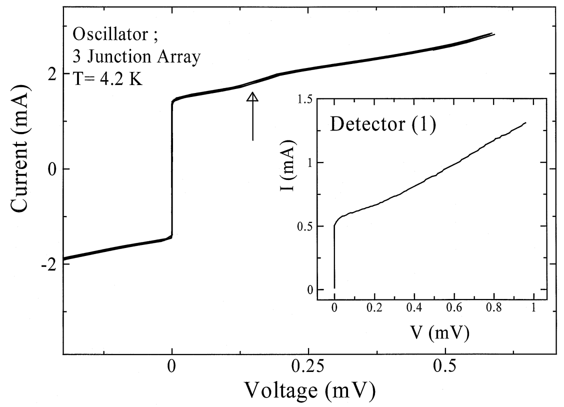

Fig. 2. I–V characteristic of the array junction and the detector junction (a). The arrow indicates the resonance step.

was usually larger than that of a single junction and conversely, the R_n value is lower. For a single detector junction, the Josephson radiation peaks according to the Josephson voltage–frequency relation were observed up to near T_c. The $I_c R_n$ product of the single detector junction was about 0.5 mV. The measured maximum radiation power was about 3–5 pW at receiving frequency $f_{REC} = 22$ GHz at 4.2 K. The measured full linewidth was about 4 GHz which deviated from the theoretical value of RSJ-model. The measured linewidths showed additional noise in the whole temperature range [9,10].

Fig. 2 shows the typical I–V characteristics of the YBCO three-junction array and the detector junction (a). We observed that both I–V characteristics were close to those predicted by the RSJ-model. We also confirmed that the Josephson self-radiation peak positions satisfied the Josephson relation. The I–V characteristic of the three-junction array exhibited a step-like resonant structure which was influenced by the frequency mode of coplanar microstrip resonator structure. The observed resonance frequency in the I–V characteristics was about 65 GHz, which is comparable to the calculated resonance frequency of 79 GHz [3]. The fundamental resonance frequency is basically influenced by the total length of resonator, the structure of the feedback loop and the microstrip lines. Note that the difference between the designed and observed frequencies is due to the difference of impedance between the coplanar resonator and the Josephson junction. Because the resonance step mode in the I–V characteristic is caused by the interaction between the high-frequency current of the Josephson junction array and the resonance frequency of coplanar microstrip resonator. However, in addition, we found that the resonant mode of the junction array was also strongly affected by the flux in the coplanar microstrip loops. The fundamental resonance frequency is basically influenced by the total length of resonator, the structure of feedback loop and the structure of microstrip lines. In addition, however, we found that the resonance mode was also strongly affected by the flux in a microstrip loop. The resonance step structure was drastically changed with varying in external magnetic field. This fact indicates that the radiation power is controllable without changing the geometrical resonance condition [8,11].

In Fig. 3, we directly compared the frequency dependent Josephson radiation power between a single detector junction (a) and a three-junction array with off-chip geometry. The power of the three-junction array was 18 pW at a receiving frequency $f_{REC} = 22$ GHz, which was almost four times larger than that of a single bicrystal junction. The results provide the evidence that the phase coherent state of the junction array was enhanced by the resonance feedback circuit. For the ideal three-junction array, if the junctions were in a phase-locking state, the maximum available power of the three-junction array would become three times larger according to $P_{max} = (1/8)NI_c^2R_n$, where N is the number of junctions

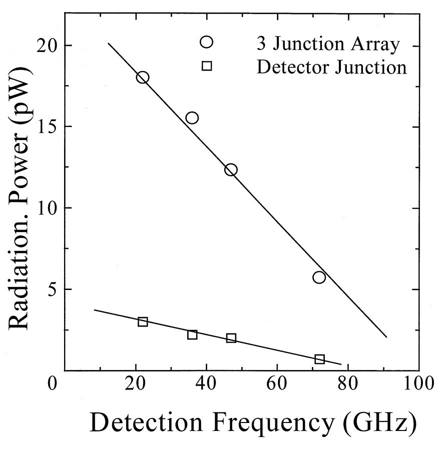

Fig. 3. Frequency dependence of Josephson radiation power for a YBCO three-junction array and a YBCO single bicrystal junction.

[3,12]. The array should deliver the maximum power of 17 nW into a matching load. In practice, however, from the theoretical estimate of mismatch between the array impedance and the load impedance of a receiver, the transmission power is found to be three orders of magnitude smaller than the above value. To improve the mismatch between the junction and the microwave receiver system, we must consider the mismatch parameters, such as the critical current and the normal state resistance of the detector and the array junctions. Note that, the junctions connected in parallel had a low junction resistance and a large critical current compared to the single junction. For the array junction geometry, the dc bias current was fed to the junction array having parallel geometry with pair of junctions shunted by the high impedance superconducting loops. The configuration of bias lead was a series of interlocking dc SQUID's geometry with the object of guaranteeing the oscillation of all junctions at the same frequency. However, one should think about the microwave impedance connected in series. A feasible way of matching is to use series array of three coherent junctions to increase the impedance. The schematic of series array is illustrated in Fig. 1(b). Note that, if the number of junctions N is chosen such as $NR_J = R_L$, where R_J is the resistance of a single junction and R_L is the load impedance, the maximum power available to the load is approximately $(1/8)I_c^2R_L$. With a matching load, the available power is proportional to N^2. However, without matching load like our case, the available power is proportional to the number of junctions. Thus, as shown in Fig. 3, our result showed a qualitative improvement of phase locking of the junction array.

To investigate the mutual phase-locking due to the influence of an array on a detector junction, we measured the I–V curves of the detector junction with the array junction biased at a certain fixed current with on-chip geometry. The detector current was swept independently. Fig. 4 shows the I–V curves of the detector junction at different array bias currents. The first Shapiro step of the detector junction appeared at the same bias voltage of the three-junction array at a given bias current. To provide a better view, the I–V curves are displaced along the current axis. The arrow indicates the first self-induced Shapiro steps caused by the oscillation of the

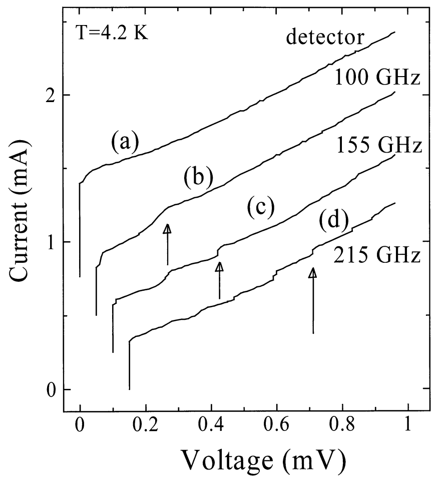

Fig. 4. I–V characteristics of the detector junction at different array bias currents (a) 0 mA, (b) 1.65 mA, (c) 1.85 mA and (d) 2.15 mA. The arrows indicate the first self-induced Shapiro steps in the detector junction.

three-junction array. At this temperature, the critical current and the normal resistance of the junction array were $I_c = 1.25$ mA and $R_n = 0.31$ Ω, respectively. In all these I–V curves, the first Shapiro step is clearly visible. In addition, higher steps and subharmonic steps were also visible. The inclined Shapiro step at array bias current $I_b = 1.65$ mA indicates that the array in this particular state does not radiate a phase-locked single emission but rather a broad band emission, as shown in the curve (b) in Fig. 4. By varying the array bias current, the main Shapiro step in the detector I–V curve was sharpened. The first Shapiro step can be shifted from 200 mV up to 500 mV, corresponding to the frequency range from 120 GHz to 240 GHz, respectively.

To determine the detected microwave emission power, we estimated the power directly from the step height of I–V curve using the analytical formula based on the RSJ model. It is possible to calculate the power from the height of the first Shapiro step according to the formula $P = 0.5(II_\omega/I_c)^2 R_{det}$, where I is the bias current, I_ω is the height of first Shapiro step and R_{det} is the detector junction resistance [3,13]. The power calculated using this formula is about 6.6 nW at 180 GHz. The maximum power of the three-junction array delivered to the detector junction by assuming that the junctions are in phase-locked is about 17 nW according to the formula $P_{max} = (1/8)NI_c^2R_n$. The detected power from the detector junction is three times smaller than that of the theoretical value. However, if we take into account the losses and reflection in the microstrip line due to impedance mismatch, the measured value using the detector junction is almost consistent with the expected value.

The detected power of radiation from the array as a function of the dc bias on the array is shown in Fig. 5. The maximum detected microwave power level was about 7 nW at frequency 200 GHz. The frequency characteristics of the detected power in a small voltage range below 0.3 mV exhibited a broad locking behavior affected by internal noise arising from the incoherent microwave emission properties of the three-junction array. The structure of induced steps at high voltages was rather complicated and could be identified due to the multiple interaction between harmonics.

Note that the radiation properties and the resonance structure of the junction array shunted by superconducting SQUID loops could be modulated by the external magnetic field to the junction array. In practice, it is very difficult to maintain the same flux through all the SQUID loops of the junction array. However, by applying a small magnetic field to the junction array, it is possible to stabilize the maximum available radiation. Without magnetic field, the relatively broad radiation peak appears.

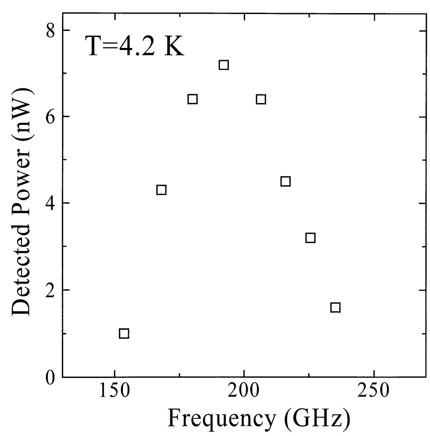

Fig. 5. Detected power of radiation from an array junction oscillator as a function of different bias levels in terms of frequency for the array junction.

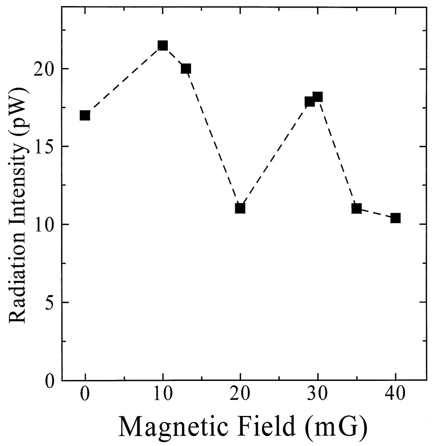

Fig. 6. Magnetic field dependence of the Josephson radiation power at receiving frequency $f_{REC} = 11.6$ GHz for a YBCO three-junction array.

With a weak magnetic field of $B = 10$ mG, however, the Josephson emission peak intensity increases and the linewidth becomes narrow. The radiation power from the array varied as a function of applied flux. The dependence of the locking properties by applying an external magnetic field is shown in Fig. 6. The approximately periodic dependence of the locking interval on magnetic field is a manifestation of the periodic dependence of the stability of the phase-locked state on magnetic field. The modulated percentage of the radiation power and the linewidth from the array by the magnetic field was about 30% for both. The measured minimum linewidth of the junction array was about 700 MHz which could not be achieved by a single bicrystal junction.

5. Summary

We have observed the mutual phase interaction between a single detector junction and a phase-locked three-junction array of HTSC Josephson junctions. In the array structure, we directly measured the radiation power of the Josephson-junction array using off-chip geometry coupled to a radiometer and on-chip geometry coupled to the detector junction. Clear self-induced Shapiro steps were observed in the current–voltage curves of the detector junction caused by the interaction with the array junction. The power transfer to the single detector junction was of the order of nW at frequency 150–250 GHz. Our circuit demonstrated the evidence of a strong phase-locking and showed the qualitative agreement with the theoretical available power by taking into account the mismatch and losses. These results may provide the optimum pumping condition for the oscillator to operate the Josephson detector junction. To demonstrate the self-pumping HTSC one chip Josephson mixer, a junction array coupled with detector Josephson junction-mixer is under investigation.

References

[1] J. Edstam, H.K. Olsson, Appl. Phys. Lett. 64 (1994) 2587.
[2] C.D. Reintsema, R.H. Ono, T.E. Harvey, N. Missert, L.R. Vale, Appl. Phys. Lett. 62 (1993) 637.
[3] A.K. Jain, K.K. Likharev, J.E. Lukens, J.E. Sauvageau, Phys. Rep. 109 (1984) 309.
[4] J.E. Lukens, Superconducting Devices, Academic Press, San Diego, 1991.
[5] G. Kunkel, G. Hechtfischer, M. Frommberger, K. Veit, R. Kleiner, P. Muller, E. Prusseit, H. Kinder, R.H. Ono, IEEE Trans. Appl. Supercond. 7 (1997) 3339.
[6] J. Edstam, G. Brorsson, E.A. Stepantssov, H.K. Olsson, IEEE Trans. Appl. Supercond. 5 (1995) 3276.
[7] G. Kunkel, R.H. Ono, Appl. Phys. Lett., 69 (199) 1960.
[8] K. Lee, I. Iguchi, J. Kim, S. Han, K. Kang, IEEE Appl. Supercond. 7 (1997) 3399.
[9] K. Lee, I. Iguchi, Appl. Phys. Lett. 66 (1995) 769.
[10] W. Reuter, M. Siegel, K. Herrmann, J. Schubert, W. Zander, A.I. Braginski, Appl. Phys. Lett. 62 (1993) 2281.
[11] K. Lee, I. Iguchi, K.Y. Constantinian, G.A. Ovsyannikov, J. Kim, K. Kang, IEICE Trans. Elect. E80 C (1997) 1275.
[12] R.D. Sandell, C. Varmazis, A.K. Jain, J.E. Lukens, AIP Conf. Proc. 44 (1978) 327.
[13] K.K. Likharev, Dynamics of Josephson Junctions and Circuit, Gordon & Breach, New York, 1986.